

Biomechanical Analysis of the Crystalline Lens Complex: A Computational Model

Leonor Jud
leonorjud@tecnico.ulisboa.pt

Instituto Superior Técnico, Universidade de Lisboa, Portugal

October 2021

Abstract

In the context of the study of the crystalline lens complex and its disorders, the present study was developed with the objective of comprehending the relevant features that can lead to the worsening of an individual's visual capacity. The condition of pseudoexfoliation, prevalent in up to 30% of individuals older than 60-years-old, can lead to severe conditions such as subluxation or dislocation of the lens, due to the weakening of the zonules. Models for a 62-year-old lens complex were developed, composed by the capsular bag, cortex and nucleus and anterior, equatorial and posterior zonular fibres. Healthy and pseudoexfoliative conditions were assessed for the lens complex, and the measurement of the visual capacity of the lens was measured in both cases. The present work aims to diminish the knowledge deficit in the subject of zonulopathy, providing vital data in the understanding of the effects of pseudoexfoliation from an optical and a biomechanical perspectives.

Keywords: Crystalline lens, Pseudoexfoliation Syndrome, Zonular Fibers, Capsular Bag, Finite Element Method

1. Introduction

The human crystalline lens allows the transmission and convergence of the light received by the eye into the retina, and is a vital optical component of the human eye. Additionally, the change in shape of this component, with the support of the surrounding structures, allows for the variation between near and distant visions.

The present work aims to evaluate the biomechanical and optical behaviours of the healthy lens complex, as well as depict the effects of zonulopathy in the lenticular system, in particular, under conditions of the pseudoexfoliation syndrome.

In the context of the human eye, this syndrome is characterized by the pathological production and accumulation of an abnormal fibrillar extracellular material in ocular tissues, such as the lens capsule and the ciliary processes. The syndrome can be timely detected when observing the presence of the white pseudoexfoliative material in the anterior surface of the lens capsule.

Pseudoexfoliation affects up to 30% of people older than 60-years-old in a worldwide distribution [1]. Under these circumstances, 70 million individuals are estimated to live with this condition. This age-related disease is often correlated with cataract and glaucoma conditions [2]. Additionally, the risk of conditions such as spontaneous subluxation or

dislocation of the lens can be up to ten times higher than for the case of healthy eyes [1]. Other risks associated with this disease are the conditions of phacodonesis and, during surgery performed on the lens complex, further zonular dialysis and vitreous loss.

As such, the need to understand the biomechanical behaviour of the eye with such a condition becomes prevalent, since the biomechanical effects of this disease can bring awareness related to the severity of the zonular dialysis and the best way to approach it, in a surgical context.

2. Background

2.1. The healthy lens complex

The crystalline lens is placed in the anterior segment of the eye, posterior to the iris and anterior to the vitreous body. The lens is composed by its cortical and nuclear regions and is contained by an elastic membrane, also known as the capsular bag. This structure is then connected to the main ocular architecture by the zonular fibers i.e., the suspensory ligament of the lens, which originate on the ciliary muscle. The fibers are divided in three different sets: the anterior, equatorial and posterior zonule.

In regards to the change of the lens shape, the most unanimous theory that explains the accommodation mechanism is presented by Helmholtz.

The author’s understanding of the change of focus provided by the lens states that the near vision is achieved in the accommodated state and is obtained due the contraction of the ciliary muscle, that relaxes the zonular fibers and leads to the increase of curvature of the lens. On the contrary, when the distant vision state is achieved, the ciliary muscle is relaxed, causing the zonular fibers to stretch and the consequent elongation of the lens.

However, the lens is subjected to changes in its structure throughout the life of the individual, and as the lens ages, its ability to accommodate decreases significantly [3]. The central optical power calculation provides a way to quantify the accommodative power of the lens, in dioptres (D), and is represented in Equation 1.

$$COP = \frac{n_l - n_p}{r_a} + \frac{n_l - n_p}{r_p} - \frac{t \cdot (n_l - n_p)^2}{r_a \cdot r_p \cdot n_l} \quad (1)$$

Where $n_l = 1.42$ stands for the equivalent refractive index of the lens and $n_p = 1.336$ the refractive index of the aqueous humour and vitreous body. Variable t represents the total thickness of the lens and r_a and r_p are the anterior and posterior radii of curvature, respectively. The amplitude of accommodation, that measures the dioptric power difference between the accommodated and relaxed states of the lens is represented as ΔCOP .

According to the estimations by [4], the accommodation amplitude of the lens, ΔCOP , reaches a value of $9.5D$ at 20 years-old and gradually loses this capacity, achieving $3.7D$ at 45 years and $1.0D$ at 60 years of age.

2.2. Pseudoexfoliation syndrome

The presence of the pseudoexfoliation syndrome in the lens complex leads to the proliferation of the material bundles in the ciliary processes and the pre-equatorial lens epithelium. These regions are also locations of zonular fiber insertion, leading to the deposition of the degenerative material in these fibers, promoting zonular dialysis and weakness: the fibers are locally lifted off from the lens capsule and ciliary muscle, leading to their rupture due to the outburst of degenerative material [1, 5, 6].

Findings related to the location of the zonular dialysis reported that the zonular dialysis can be present in the inferior and superior regions of the structures [7], and that deposition of the pseudoexfoliative material is performed in the antero-posterior direction [5, 8].

The zonular weakness was also characterized according to the term clock-hours, which reflect the extension angles of zonulopathy, with each clock-hour accounting for a 30 degree zonular section. Different levels of zonular fiber extension were

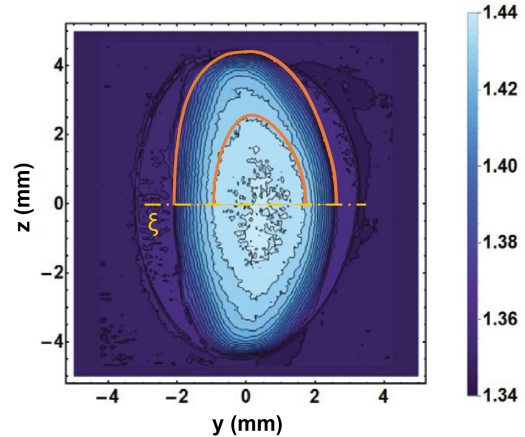


Figure 1: Refractive index contours and geometrical parameters of the lenticular components [11].

found, where the dialysis could extend for 3 contiguous clock hours (90 degrees), 6 clock hours (180 degrees) and throughout the whole zonular structure (360 degrees) [9].

The effect of pseudoexfoliation in the accommodative capacity of involved eyes was investigated, and the study reported that the accommodative capacity decreased significantly in patients with pseudoexfoliation, when compared to healthy lenses [10].

3. Materials and Methods

3.1. The Healthy Lens Complex

With the objective of studying the human lens at an age where there would be a significant prevalence of the pseudoexfoliation syndrome, a three-dimensional 62 years-old lens was modelled. The geometries of the nucleus and cortex of the lens were designed taking as a baseline the refractive index contours of the 62 year lens [11]. The resulting geometries are depicted in Figure 1, where the outer profiles of the nucleus and cortex were used to create axisymmetric structures, recurring to the axis of revolution ξ . These structures were modelled with 4-node linear tetrahedral elements, recurring to the Abaqus [®] (Dassault Systèmes, France) software.

The capsular bag was designed as a membrane enveloping the cortex and, therefore, its geometry was constructed taking into account the outer profile defined for the cortex. The capsule’s thickness was defined with a dimension of $T_{CB} = 20\mu m$, uniformly defined throughout its structure [12]. The capsule was modelled with 3-node triangular shell elements.

The zonular length of the three sets of zonules was $l_Z = 1.5mm$, and the defining angles of the zonular sets were $\alpha_{ZA} = -10deg$, $\alpha_{ZE} = 0deg$ and $\alpha_{ZP} = 24deg$ for the anterior, equatorial and zonu-

lar fibers, respectively [12]. The three sets were defined with the same thickness value ($T_Z = 10\mu m$) [13]. The three zonular sets were modelled with 3-node triangular membrane elements.

The lenticular components and the capsular bag were considered as having linear elastic isotropic material properties, and being quasi-incompressible structures. Accordingly, the Young's moduli of the cortex and nucleus were $E_C = 0.04kPa$ and $E_N = 0.82kPa$, and having the same Poisson coefficient ($\nu_C = \nu_N = 0.47$) [12], whereas the capsular bag had the following material parameters: $E_{CB} = 1.5MPa$, $\nu_{CB} = 0.47$ [12, 14]. The zonular fibers were modelled as hyperelastic anisotropic structures [15], according to the constitutive properties based on the Holzapfel-Gasser-Ogden model[16]. The resulting material constants of the zonules that describe their constitutive behaviour were $C_{10} = 0.0583$, $D_1 = 1.0286$, $k_1 = 0.087MPa$, $k_2 = 21.75$ and $kappa = 0.3$.

The boundary and interaction conditions imposed in this work related to the connection between structures, where the exterior surface of the nucleus was tied to the cortex interior facet, and the exterior surface of the latter structure was connected to the capsular bag's interior membrane surface. A connection was also enforced between the interior edges of the zonules and the external insertion regions of the capsule. The most anterior and posterior poles of the lenticular components were only allowed movement in the optical axis direction, and the zonular movement was restricted in all directions with the exception of the radial one. The disaccommodation process was simulated taking into account the displacement of the exterior edge of each of the zonular sets, $\delta_Z = 0.5mm$, that were stretched in the radial direction [12].

Zonular fiber geometry The geometry of the zonules was then varied, given that these structures can have up to 5.6% difference between vertical and horizontal lengths, where the latter have a smaller dimension. Accordingly, models were designed taking into account the representation depicted in Figure 2, and the measurements of the resulting zonular lengths are laid out in Table 1. As the models progress, there is an increase of the average fiber length, $\overline{l_Z}$.

Capsular bag attachment Additionally, the study of the boundary conditions related to the capsule and zonules was assessed. With the objective of avoiding the numerical kinks originated by the zero-width rings [17] and understanding the impact of the insertion band width in the models, master surfaces were created in the capsule, portraying the belts of anchorage of the zonules, and allowing for the connection between the referred components. The models developed are represented in Table 2,

Model	Vertical length	Horizontal length
	$l_{Z_V}[mm]$	$l_{Z_H}[mm]$
Oval-5.6	1.500	1.416
Oval-2.8	1.500	1.458
Initial Model	1.500	1.500
Oval+2.8	1.542	1.500
Oval+5.6	1.584	1.500

Table 1: Models developed to assess the geometry of the zonular fibers.

where models *Band3* and *Band7* have a band width correspondence with literature values [17, 18], and the remaining models evaluate the intermediary values between the forementioned band widths.

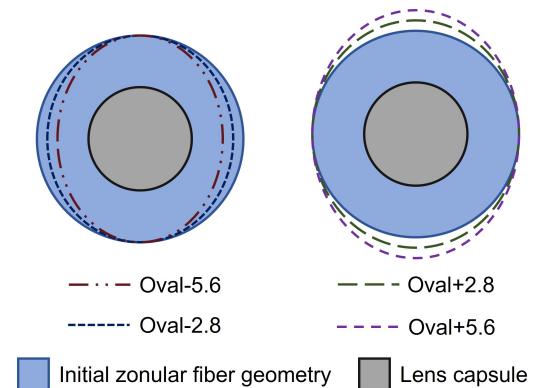


Figure 2: Geometrical configurations of models

The gravitational force impact in the lens complex was assessed, where the density values of cortex, nucleus and capsule were equivalent ($\delta_C = \delta_N = \delta_{CB} = 1099kg/m^3$) [19], and the density of the zonules was determined as $\delta_Z = 1000kg/m^3$ [20].

3.2. Pseudoexfoliation Syndrome

The condition of zonular dialysis was simulated taking into account the thickness reduction of the zonular set of fibers, due to the local lifting off of a portion of the fibers, whether it be from the ciliary muscle of the lens capsule [5]. Two cases of zonular fiber separation were considered. A moderate situation, where 50% of the fibers were disconnected, leading to a resulting thickness of the afflicted areas of $T_Z = 5\mu m$ and a severe case, where the critically affected areas had 5% of healthy zonular thickness ($T_Z = 0.5\mu m$) with transitional regions of moderate dialysis, where $T_Z = 5\mu m$.

Taking into consideration the antero-posterior direction of the zonulopathy conditions [5, 7], the anterior zonules, the group of anterior and equatorial fibers, and the group of three sets of zonular fibers were degenerated. Nonetheless, for the sake of the individual characterization of the each fiber

Model	Anterior Band Width $\Delta y_{CB-ZA}[mm]$	Equatorial Band Width $\Delta y_{CB-ZE}[mm]$	Posterior Band Width $\Delta y_{CB-ZP}[mm]$
Band1	0.167	0.167	0.133
Band2	0.333	0.333	0.267
Band3	0.500	0.500	0.400
Band4	0.590	0.590	0.548
Band5	0.680	0.680	0.695
Band6	0.770	0.770	0.843
Band7	0.860	0.860	0.990

Table 2: Band widths of the capsule’s anchorage regions for different model configurations.

set, the individual dialysis of the equatorial and posterior fibers was also modelled.

Given the fact that zonulopathy can either occur in the inferior or superior regions of the zonules [7], these two cases were simulated. Upon modelling the extension of zonular dialysis, the degeneration was accounted for 1, 3, 6, 9 and 12 clock hours, which corresponded to angles of 30, 90, 180, 270 and 360 degrees of zonulopathy.

Figure 3 portrays the schematic representation for the superior dialysis of the anterior zonules, for moderate and severe cases and for all angle cases of zonulopathy extension. Taking into account the progression of the pseudoexfoliation syndrome with regards to the previously mentioned factors, a total of 90 models were developed, in order to depict a gradual and progressive advancement of the disease in the lens complex.

3.3. Procedures for Result Analysis

With the goal of facilitating the result analysis process, a script was developed in Python [®](Python Software Foundation, Delaware, USA), where several data outputs were collected, throughout the lens deformation, which was divided in six equal increments [17]. The results include the lens thickness variation, ΔT_L , lens radius variation, ΔR_L total zonular force, F_Z , the capsular bag strain and stress ranges found for all the components. The Central Optical Power was also calculated for all models, throughout the six simulation steps defined for the disaccommodation process [17]. This quantity was measured in the sagittal plane of the lens, where the radii of curvature were calculated assuming that the anterior and posterior surfaces of the lens were spherical.

4. Results and Discussion

4.1. The Healthy Lens Complex

The lens under the initial conditions flattened $\Delta T_L = 14.20\%$ and its radius increased $\Delta R_L = 7.87\%$ during the disaccommodation process. The force acted on the zonular fibers was totaled as $F_Z = 134.1mN$. The logarithmic strain endured by the capsular bag, LE_{CB} , ranged from $1.66E - 2$ to

$8.25E - 2$. The principal stress values found for the capsular bag in the validation model ranged from $41.53kPa$ to $171.59kPa$, given that the regions under a greater amount of stress are the capsular bag’s anchorage rings, which connect to each of the zonular fiber sets. The stress in the nucleus and cortex was evaluated simultaneously, and values found for the principal stress on the structures ranged from $-0.654kPa$ to $0.841kPa$.

On the other hand, the Von-Mises stress ranged from $0.018kPa$ to $0.210kPa$, and the stress distribution showed a greater stress magnitude in the regions proximal to the capsule’s attachment rings of the zonular fibers. This result shows a stress response of the cortex to the displacement of the fibers enforced in the disaccommodation process. The resulting amplitude of accommodation of the initial model was $\Delta COP = 1.57D$ and the Central Optical Power shows an increase in the first and second steps of the lens deformation, and a reduction throughout the rest of the disaccommodation process.

Zonular fiber geometry The evaluation of the geometry of the zonular fibers results revealed that the amplitude of accommodation of the lens showed a reduction throughout the evolution of the models presented in Table 1. For the model with the smallest average fiber length, *Oval-5.6*, the amplitude of accommodation had the highest value, $\Delta COP = 2.03D$. From then on, the amplitude of accommodation decreased, reaching the lowest value in model *Oval+5.6*, where $\Delta COP = 1.38D$. The zonular force also denoted a reduction with the progression of the models in Table 1, reaching a minimum value of $F_Z = 129.9mN$, for model *Oval+5.6*. Given that these values were in a greater accordance with available literature [18, 21], *Oval+5.6* depicted an optimized geometrical parameter model, being then selected to continue the process of optimization, regarding the capsular bag attachment parameter choice.

Capsular bag attachment The evaluation of the interaction conditions, where the width of the capsular bag anchorage regions was varied, did not

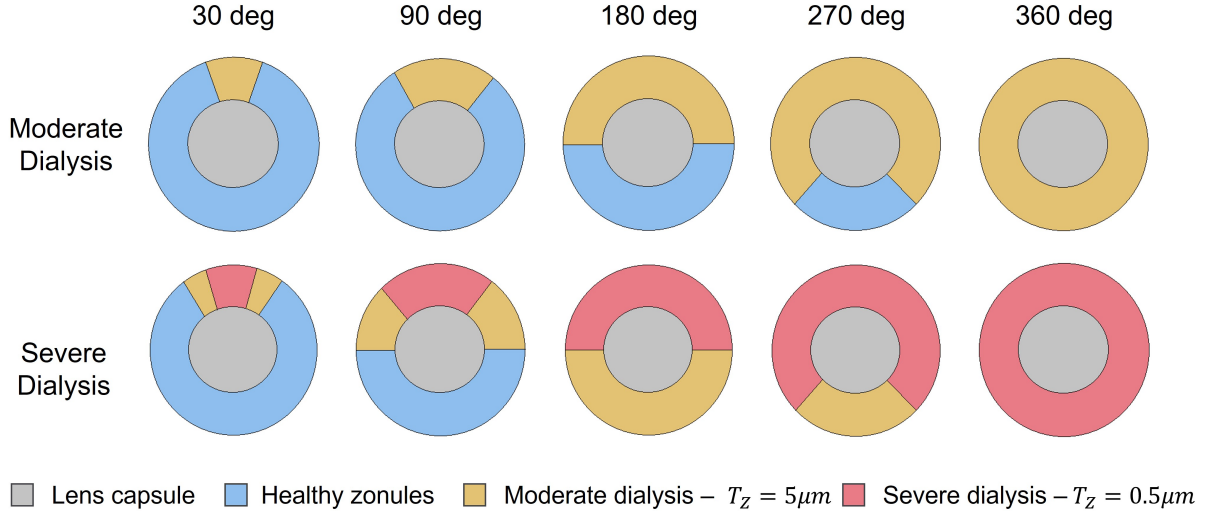


Figure 3: Frontal view schematic of the models with superior zonular dialysis.

present relevant results, given that all the models, from *Band1* to *Band7*, showed similar behaviours, both in the stress and strain endured by the components of the lens complex and the accommodative capacity of the lens, as well as the force endured by the zonular fibers. Nonetheless, all these models showed a reduction in the accommodative amplitude and zonular force when compared with the model with zero-width rings of attachment in the capsule, given that there was a reduction of the endured effort in the capsule with the imposition of anchorage bands. As such, the selected model, that portrayed optimized conditions was *Band4*, given its proximity with literature values [18, 21].

4.2. Pseudoexfoliation Syndrome

Lens thickness variation, ΔT_L : The pseudoexfoliation syndrome led to the reduction of the capacity of the lens to change its geometry. Accordingly, the lens thickness variation reduced as the syndrome progressed. The evaluation of the individual impact of each of the zonules in the thickness variation of the lens, showed that the equatorial zonules have the lowest impact in this quantity, both when moderately and severely dialysed. The posterior and anterior zonules, when considered individually, lead to the same decrease of thickness variation of the lens ($\Delta T_L = 8.55\%$ for severe dialysis cases throughout the structure of the lens). Applying a severe degeneration in all zonular sets lead to the most prominent discrepancy in lens thickness variation, given that for 360 degree dialysis this measurement was valued only $\Delta T_L = 4.28\%$.

Lens radius variation, ΔR_L : When accounting for the lens radius variation results, contrarily to the analysis of the lens thickness variation, it was noted that the equatorial zonules play now an important

role in the variation of the lens equator radius. This is due to the location of the equatorial fibers i.e., in the plane of the equator of the lens, where its radius is measured. The severe disruption of the equatorial fibers denotes a greater variation in the lens equator change in radius. When disrupted in the 12 clock hours, the lens radius variation presents a value of only $\Delta R_L = 4.64\%$. As such, this set of fibers has a greater impact in the lens radius variation than the other two individual sets of zonules, the anterior and posterior zonules.

For the case of severe dialysis of the fibers, both the anterior and posterior zonules, when considered individually, show no effect in the radius variation of the lens. The moderate zonular disruption of all the considered zonular sets, does not have a great impact in the radius variation of the lens, even when applied to the complete structure of the zonules (360 degrees). For the three sets of zonules, when moderately afflicted throughout their complete structures, the lens equator shows a variation of $\Delta R_L = 6.42\%$, a reduction of 1.52% from the value found for the healthy model.

Accommodation amplitude, ΔCOP : The accommodation amplitude results are depicted in Figure 4. The figure comprises the dialysis of the anterior zonules (*ZA*), equatorial zonules (*ZE*) and posterior ones (*ZP*), when degenerated in moderate (represented by the term 50%) and severe (5%) conditions. As for the case of 0 degree degeneration, the model *Band4* is portrayed with gravitational conditions, that were applied to all the pseudoexfoliation models. When evaluating the singular impact of the equatorial zonules in the accommodative capacity of the lens, one can recognize that both when moderately and severely dialysed, the amplitude of accommodation attained by the lens shows

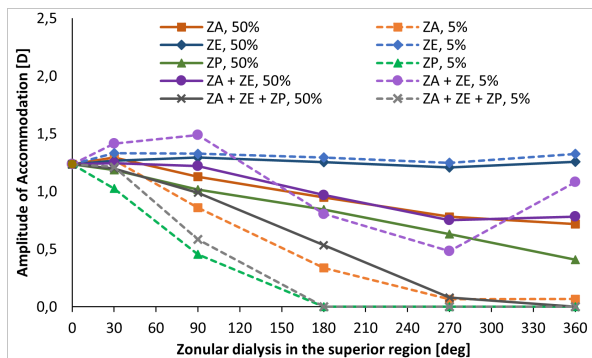


Figure 4: Amplitude of accommodation of the lens for pseudoexfoliation models with superior dialysis.

no significant reduction for all cases of dialysis extent. Considering the singular performance of the dialysed anterior fibers, when moderately afflicted, there is a reduction of the accommodation amplitude as the extent of dialysis increases, reaching a minimum value of $\Delta COP = 0.72D$ for the fully afflicted anterior fibers i.e., throughout their complete structure. The moderate dialysis of the three zonular sets leads to the most acute reduction of accommodative amplitude in the models with 50% zonular thickness. The accommodation amplitude decreases significantly when increasing the dialysis degree, reaching a value of 0.08 dioptres in the case with 270 degree dialysis, and 0 dioptres when all zonular sets are completely disrupted.

Total zonular force, F_Z : The results found for the total force endured by the zonules during the deformation of the lens denote that all types of degeneration showed a downward slope in the resulting zonular force, as the extension of dialysis progressed from 30 degrees upwards. The zonular force due to the displacement of the fibers has a greater value in the exterior edge of the zonules, since this is the location of the boundary condition enforced on the fibers.

Capsular average Von-Mises stress, \overline{VM}_{CB} : Due to the deteriorated conditions of the zonules, their stretching does not cause the same deformation on the capsule, which then translates to a reduction of the amount of stress that the capsule is under. Since the areas of greater stress in the capsule are the attachment regions to the anterior, equatorial and posterior zonular fibers, as these components are thinned, the same displacement of the remaining fibers does not cause the same behaviour in the capsule. The moderate disruption of each of the zonules led to a small decrease of the average stress endured by the capsule. The most extreme of the cases was for the moderate disruption of the anterior zonules, with $\overline{VM}_{CB} = 64.7kPa$, for 360 degree dialysis. The analysis of cases with severe zonu-

lopathy led to the following deductions: the equatorial zonules are the ones with the lowest impact in this quantity, followed by the posterior zonules. The anterior zonules are the ones that, individually, cause the capsular bag to endure the smallest value of average Von-Mises stress, when dialysed. The curve denoting a severe disruption of the anterior and equatorial fibers had a downward slope throughout the extension progression of dialysis, although more pronounced for the first 180 degrees of extension. From then on, the slope showed a more lenient inclination, and at 360 degrees dialysis, the average stress endured by the model with zonulopathy of anterior and equatorial fibers was $VM_{CB} = 35.0kPa$.

Zonular maximum Von-Mises stress, $max(VM_Z)$:

The maximum value of Von-Mises stress that the zonules endure during disaccommodation of the lens is depicted in Figure 5. The models that accounted for severe dialysis of the zonules all showed a significant increase of the maximum zonular stress, with the exception of the equatorial zonules. Accordingly, the individual disruption of the anterior fibers showed a similar behaviour to the one of the individual posterior fibers, where there was an increase of the maximum stress endured by the zonules up to 270 degree dialysis extension, followed by a reduction from the forementioned cases to the ones with 360 degree dialysis. The same results were found for the cases of dialysis of the groups of zonules ($ZA + ZE$ and $ZA + ZE + ZP$), where an increase of stress was observed up to 270 degree dialysis extension, and a reduction observed for the dialysis of the whole structure. For the case of the severe disruption of the anterior and equatorial zonules, the maximum Von-Mises stress for 270 degree and 360 degree zonulopathy extensions was valued $max(VM_Z) = 1429kPa$ and $max(VM_Z) = 881kPa$, respectively. When examining the zonular areas that endured the greater amount of stress when under pseudoexfoliative conditions, the case of severe disruption of the anterior zonules was analysed, for 90 degree extension. The 90 degree region with severe disruption of the zonular fibers, where $T_Z = 0.5\mu m$, is the one that endures the greater amount of stress, in particular, in the area proximal to the capsular bag attachment. The areas of moderate disruption on both sides show a reduction of the stress endured, when compared with the severely damaged region. Lastly, the healthy region of zonules had the smallest amount of stress concentration. Nonetheless, the healthy region denotes a greater stress concentration in the areas closer to the moderately dialysed regions. These results suggest that the stress endured by the diseased regions propagates to the healthy zonules, which then causes a progression of the degeneration, given that

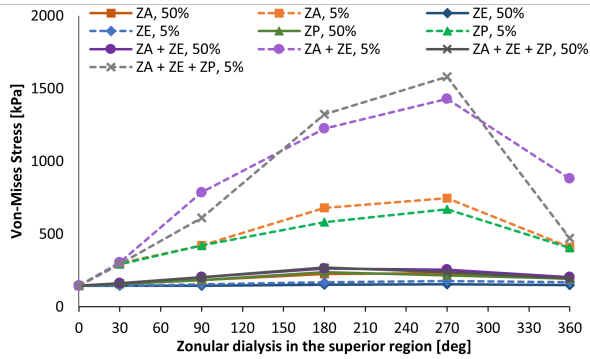


Figure 5: Maximum Von-Mises stress in the zonules for pseudoexfoliation models with superior dialysis.

the latter fibers are now under a greater amount of stress that expected in healthy conditions.

Lens maximum Von-Mises stress, $max(VM_{C+N})$: There was an overall reduction of the stress endured by the cortex and nucleus, as the pseudoexfoliation syndrome evolved and reached more advanced stages. The analysis of the equatorial fiber disruption shows that although the moderate dialysis does not cause a significant decrease in the stress endured by the lens, the severe zonulopathy of the equatorial zonules has one of the most significant impacts in the stress reduction endured by these components. The anterior zonule disruption has an inverse effect in the cortical and nuclear stress, since its dialysis leads to an increase of the resulting maximum stress.

Comparison of inferior and superior dialysis: In order to understand the relevant disparities between the two groups of models (with inferior and superior dialysis), an approximation error was computed between superior and analogous inferior models, resorting to Equation 2.

$$\lambda[\%] = \frac{value_{inf} - value_{sup}}{value_{sup}} \cdot 100 \quad (2)$$

Note that the presented variable can have negative values: when the referred value for the inferior dialysis is smaller than the superior one, λ has a negative value, in order to highlight this behaviour. The results found for the lens thickness variation, lens radius variation, and average capsular stress showed a negligible difference between models with superior and inferior origins.

The total zonular force had higher values for all the cases where there was a superior dialysis i.e., the approximation error had negative values for all the comparisons between inferior and superior cases. The average approximation error was $\bar{\lambda} = -1.6\%$. These results show that when there is a degeneration with a superior origin, the zonular fibers endured a greater amount of force when achieving the

same displacement as an analogous lens complex with inferior zonulopathy.

The most important differences between the two types of degeneration were observed in the maximum Von-Mises stress endured by the zonules, the maximum Von-Mises stress endured by the lenticular components and last but not least, the accommodation amplitude. These results are represented in Figure 6.

The average approximation error for each of the zonular groups considered denoted that the stress endured by models with superior dialysis origin endured a greater amount of stress than the analogous models with inferior dialysis origin, as defined by the negative values of $\bar{\lambda}$. These results imply that the zonulopathy causes a greater amount of stress in the zonules when its origin has a superior location. Consequently, since the healthy zonular fibers suffer a greater disruption as the stress magnitude increases, the same fibers would be under a greater degeneration when in the presence of a superior dialysis, when compared with the analogous case of inferior dialysis.

The analysis disparity between the superior and inferior values of the maximum Von-Mises stress in the cortical and nuclear components of the lens is also depicted in Figure 6. The anterior zonular fiber disruption showed a peculiar behaviour, when compared with the rest of the zonular sets: the average approximation error between superior and inferior values was valued as $\bar{\lambda} = -2.5\%$, denoting that the superior dialysis caused a greater stress in the cortex and nucleus than the inferior dialysis. However, all the other sets had an opposite behaviour, where the average approximation error was positive, showing a greater stress in the models with inferior dialysis than models with a superior one.

Last but not least, the impact on the amplitude of accommodation was compared between inferior and superior dialysis for the different zonular fiber evaluations. The equatorial fibers, given that they have no significant impact in the accommodative capacity of the lens, as can be observed in Figure 4, did not present a significant difference between the inferior and superior dialysis values, given that their approximation error was $\bar{\lambda} = 0.4\%$.

The results found for both the maximum Von-Mises stress in the zonules and the accommodation amplitude of the lens point to the same deduction, that the superior dialysis leads to a most severe degeneration of the zonules and the visual capacity of the lens. The inferior dialysis leads to a less severe reduction of the accommodation amplitude of the lens and the inferior dialysis presents smaller stress magnitudes in the zonules, which then leads to a less severe progression of the zonulopathy condition.

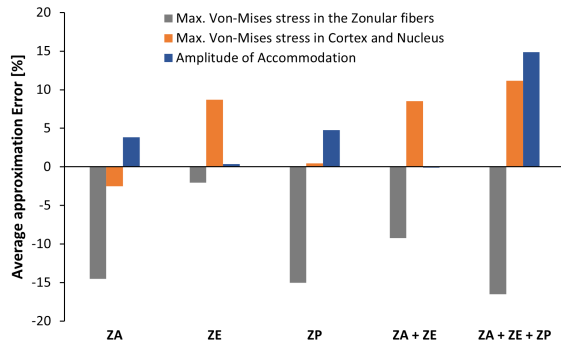


Figure 6: Comparison between superior and inferior models

5. Conclusions

The main objective of this work was to address the challenge of determining the biomechanical and optical behaviour of the human lens complex under healthy and diseased conditions.

The first part of this goal involved the construction and validation of *in silico* experiments concerning the healthy human lens and its surrounding structures.

This initial validation then led to the design of a novel 3D model for the healthy lens complex, where the biomechanical effects of both geometrical changes in the zonular fibers and the boundary conditions of the capsular bag were assessed. The variation of the assessed geometrical parameters of the zonules, where the vertical length of the fibers was 5.6% greater than the horizontal one, led to results that are more relevant in terms of the accommodative capacity and biomechanical behaviour of the lens. The assessment of the boundary conditions of the capsular bag, where the anchorage regions to the zonules were altered, led to the conclusion that when there is a zero-width insertion ring as the surface of attachment to the capsule, the values of force and accommodative amplitude are greater than for the cases where the capsule has bands of insertion with width greater than zero.

The second part of the objective defined was the analysis of the biomechanical behaviour of the lens under diseased conditions, in particular, due to the pseudoexfoliation syndrome.

The outcomes related to the pseudoexfoliation syndrome showed a significant impact of this disease in the accommodative capacity of the lens, exhibiting a complete nullification of the accommodation amplitude for the most severe cases of zonular dialysis.

The results found for this matter showed that the location of the zonulopathy in the lens complex has a significant impact in the progression of the disease and the accommodative capacity of the lens:

the superior dialysis presents optimal conditions to further the dialysis of the fibers and reduce the accommodative amplitude of the lens, when compared with the inferior dialysis location. Accordingly, the accommodative capacity of the inferior models was, on average, 4.7% greater than for the cases with superior dialysis. When the three sets of zonules were disrupted, this discrepancy increased significantly, reaching an average value of 14.9% for the mentioned models, and with a maximum value of 60.1%.

The work presented in this dissertation led to the development of innovative data concerning the healthy lens complex configuration, as well as the pseudoexfoliation syndrome and its effect in the studied system.

As a future work, the comprehensive study involved in the knowledge gained towards the mentioned syndrome could also be applied to other diseases of the human lens complex, such as the formation of cataract in the crystalline lens. Finally, the methodology applied towards the construction of the models in this dissertation could also be applied for cases in post-surgical perspectives, such as cataract surgery, where the nucleus and cortex are removed and substituted by an intraocular lens.

References

- [1] Robert Ritch and Ursula Schlötzer-Schrehardt. Exfoliation syndrome. *Survey of ophthalmology*, 45(4):265–315, 2001.
- [2] Catarina Pedrosa, Maria Lisboa, and Isabel Prieto. Pseudoexfoliation: The diagnosis at first sight. *Hospital Prof. Dr. Fernando Fonseca*, 4(1/2):54–55, 2016.
- [3] David A Atchison, George Smith, and George Smith. *Optics of the human eye*, volume 2. Butterworth-Heinemann Oxford, 2000.
- [4] J Ungerer. The optometric management of presbyopic airline pilots. *Unpublished MSc Optometry thesis, University of Melbourne, cited in Atchison and Smith*, 2000.
- [5] Gottfried OH Naumann, Ursula Schlötzer-Schrehardt, and Michael Kühle. Pseudoexfoliation syndrome for the comprehensive ophthalmologist: intraocular and systemic manifestations. *Ophthalmology*, 105(6):951–968, 1998.
- [6] Ursula Schlötzer-Schrehardt and Gottfried OH Naumann. Ocular and systemic pseudoexfoliation syndrome. *American journal of ophthalmology*, 141(5):921–937, 2006.
- [7] David J Wilson, Michele J Jaeger, and W Richard Green. Effects of extracapsular

- cataract extraction on the lens zonules. *Ophthalmology*, 94(5):467–470, 1987.
- [8] Ursula Schlötzer-Schrehardt and Gottfried OH Naumann. A histopathologic study of zonular instability in pseudoexfoliation syndrome. *American journal of ophthalmology*, 118(6):730–743, 1994.
- [9] Richard S Hoffman, Michael E Snyder, Uday Devgan, Quentin B Allen, Ronald Yeoh, Rosa Braga-Mele, ASCRS Cataract Clinical Committee, et al. Management of the subluxated crystalline lens. *Journal of Cataract & Refractive Surgery*, 39(12):1904–1915, 2013.
- [10] GF Yavas, F Öztürk, T Küsbeci, ÜÜ Inan, Ü Kaplan, and SS Ermiş. Evaluation of the change in accommodation amplitude in subjects with pseudoexfoliation. *Eye*, 23(4):822–826, 2009.
- [11] Barbara Pierscionek, Mehdi Bahrami, Masato Hoshino, Kentaro Uesugi, Justyn Regini, and Naoto Yagi. The eye lens: age-related trends and individual variations in refractive index and shape parameters. *Oncotarget*, 6(31):30532, 2015.
- [12] Kehao Wang, Demetrios T Venetsanos, Masato Hoshino, Kentaro Uesugi, Naoto Yagi, and Barbara K Pierscionek. A modeling approach for investigating opto-mechanical relationships in the human eye lens. *IEEE Transactions on Biomedical Engineering*, 67(4):999–1006, 2019.
- [13] GWHM Van Alphen and William Paul Graebel. Elasticity of tissues involved in accommodation. *Vision Research*, 31(7-8):1417–1438, 1991.
- [14] Henk A Weeber and Rob GL Van Der Heijde. Internal deformation of the human crystalline lens during accommodation. *Acta ophthalmologica*, 86(6):642–647, 2008.
- [15] Joana Paulino. 3d biomechanical modelling of the human lens complex under cataract surgery. Master’s thesis, Instituto Superior Técnico, 2019.
- [16] Gerhard A Holzapfel, Thomas C Gasser, and Ray W Ogden. A new constitutive framework for arterial wall mechanics and a comparative study of material models. *Journal of elasticity and the physical science of solids*, 61(1):1–48, 2000.
- [17] Kehao Wang, Demetrios T Venetsanos, Jian Wang, Andy T Augousti, and Barbara K Pierscionek. The importance of parameter choice in modelling dynamics of the eye lens. *Scientific reports*, 7(1):1–12, 2017.
- [18] EA Hermans, M Dubbelman, GL Van der Heijde, and RM Heethaar. Estimating the external force acting on the human eye lens during accommodation by finite element modelling. *Vision Research*, 46(21):3642–3650, 2006.
- [19] Alexandre M Rosen, David B Denham, Viviana Fernandez, David Borja, Arthur Ho, Fabrice Manns, Jean-Marie Parel, and Robert C Augusteyn. In vitro dimensions and curvatures of human lenses. *Vision research*, 46(6-7):1002–1009, 2006.
- [20] Zoltán Bocskai and Imre Bojtár. Biomechanical modelling of the accommodation problem of human eye. *Periodica Polytechnica. Civil Engineering*, 57(1):3, 2013.
- [21] Alexander Duane. Studies in monocular and binocular accommodation with their clinical applications. *American Journal of Ophthalmology*, 5(11):865–877, 1922.